Time-Dependent Nuclear Measurements of Mix in Inertial Confinement Fusion

Ignition and high gain in inertial confinement fusion (ICF)[1,2] are critically dependent on mitigation of the Rayleigh–Taylor (RT) instability. ICF capsules typically consist of a spherical shell filled with a gaseous fuel and are imploded using lasers (direct drive) or x rays (indirect drive) to rapidly deposit energy and ablate the capsule surface. The RT instability, which is the growth of nonuniformities at a density interface when a low-density material accelerates a high-density material, occurs during two distinct intervals in ICF implosions. During the acceleration phase, the low-density ablating plasma accelerates the solid shell inward, and perturbations seeded by energy deposition nonuniformities or initial capsule surface roughness feed through to the inner fuel–shell surface. During the deceleration phase, shortly before the time of maximum capsule compression, growth of the RT instability at the fuel–shell interface quickly saturates, resulting in small-scale, turbulent eddies that lead to atomic-scale mixing of the fuel and shell.[3] RT growth and the resulting mixing processes disrupt the formation of a hot spot in the fuel, lowering its temperature and reducing its volume, which may prevent the capsule from igniting. Understanding the nature and timing of RT growth and mix under different conditions is an important step toward mitigating their adverse effects.

Substantial and sustained efforts to understand RT instability and mix have been ongoing for many decades.[4] This article presents the first time-dependent nuclear burn measurements of the mix region in ICF implosions. Although it has been previously demonstrated that there is no mix in the burn region at shock bang time,[5,6] it was unknown how long after shock collapse it takes for atomic mixing to occur. Other relevant work on the mix region in ICF implosions includes time-integrated nuclear yield measurements in both direct-drive[6–10] and indirect-drive[11] configurations, as well as time-dependent x-ray measurements of capsules doped with tracer elements.[12] In addition, time-dependent nuclear measurements obtained from implosions of CD-shell capsules filled with nearly pure tritium have recently been reported.[13]

This article reports results from direct-drive experiments conducted with the OMEGA Laser System,[14] with 60 fully smoothed,[15] UV (λ = 351 nm) beams in a 1-ns flat-top pulse and a total energy of 23 kJ. The on-target illumination uniformity was typically ≤2% rms. The spherical plastic target capsules had diameters between 860 and 880 μm, a total shell thickness of 20 μm, and a 0.1-μm-rms outer surface roughness. "CH" capsules had plastic (CH) shells and a gaseous fill of deuterium and helium-3 (D_2 and ^{3}He, equimolar by atom). "CD" capsules had gaseous fills of pure ^{3}He and a shell made mostly of CH, except for a 1-μm layer of deuterated plastic (CD) on the inner surface (Fig. 110.62). The fill pressures of the D^{3}He and the pure ^{3}He mixtures in CH and CD capsules were chosen to give equal initial fill mass densities ρ_0 at values of 0.5 or 2.5 mg/cm^3. Because fully ionized D and ^{3}He have the same value of $(1+Z)/A$, mixtures with the same mass density have the same total particle density when fully ionized and can be considered hydrodynamically equivalent.[16]

Implosions of CH and CD capsules were observed using simultaneous measurements of products from two distinct primary nuclear reactions to study the nature and timing of mix. The D-^{3}He reaction, D + ^{3}He → ^{4}He + p, and the DD-n reaction, D + D → ^{3}He + n, have dramatically different composition and temperature sensitivities,[16] which are used herein to constrain possible mix scenarios. The D-^{3}He reaction depends much more strongly on temperature due to the doubly charged ^{3}He reactant, and when the reactant species are initially separated, such as in CD capsules, they must be mixed before nuclear production will occur.[17]

Possible scenarios of atomic mix are constrained using spectral measurements of nascent 14.7-MeV D^{3}He protons. D^{3}He protons experience energy loss from their birth energy as they pass through the compressed shell plasma on their way out of the capsule. The proton-emission, path-averaged capsule areal density ρL is inferred using the mean-energy downshift of measured proton spectra.[18] For implosions with the same mean radial areal density ρR, the value of ρL depends on the spatial distribution of the proton source and shell mass.[18] A larger correction factor is needed as the mean source radius approaches the mean shell radius, as protons traverse longer paths through the shell. For example, a quasi-one-dimensional scenario of atomic mix that consists of a spherical mixing layer just inside a compressed spherical shell will require a much larger correction factor than a three-dimensional scenario involving turbulent mix induced at the tips of RT spikes driven into the hot core.

The dynamics of RT growth are of essential importance for any mix scenario. These dynamics are studied using temporal measurements of the emission of D^3He protons, obtained using the proton temporal diagnostic (PTD).[19,20] The PTD primarily consists of a 1-mm-thick BC-422 scintillator, an optical transport system, and a fast streak camera. Optical fiducial pulses simultaneously recorded by the streak camera give an absolute timing accuracy of ~25 ps. The time history of the proton arrival at the scintillator is obtained by deconvolution of the detector response from the streak camera image. D^3He proton spectral measurements[18] are then used to infer the D-^{3}He reaction rate history from the proton current at the scintillator. Additional details on PTD instrumentation and data processing can be found in Frenje *et al.*[19]

Temporal measurements of 2.45-MeV neutrons from the DD-*n* nuclear reaction were obtained using the neutron temporal diagnostic (NTD),[21] which works on the same principle as the PTD, but is optimized for neutron detection. Although the D-D reaction rate in CD capsule implosions is below the noise floor of the NTD, integrated D-D yields were readily obtained using time-of-flight neutron detectors.[22]

Implosions of CH capsules with D^3He fuel characteristically emit D^3He protons at two distinct times (Fig. 110.62). The shock burn is induced by the collapse of an ingoing spherical shock and occurs before the imploding shell starts to decelerate. About 250 ps later, during the deceleration phase, the compression burn occurs as the imploding capsule compresses and reheats the fuel. In contrast to the two stages of proton emission observed in CH capsule implosions with D^3He fills, CD capsules emit protons only during the later phase (Fig. 110.62), confirming the hypothesis that there is no mix at the time of shock collapse,[23] first presented by Petrasso *et al.*[5]

Measurements of time-integrated nuclear yields demonstrate that capsules with lower ρ_0 have an increased susceptibility to mix.[6,9] Yields increased with lower ρ_0 for CD capsule implosions, even though low ρ_0 is less favorable for nuclear production in the capsule core, as seen through the decrease

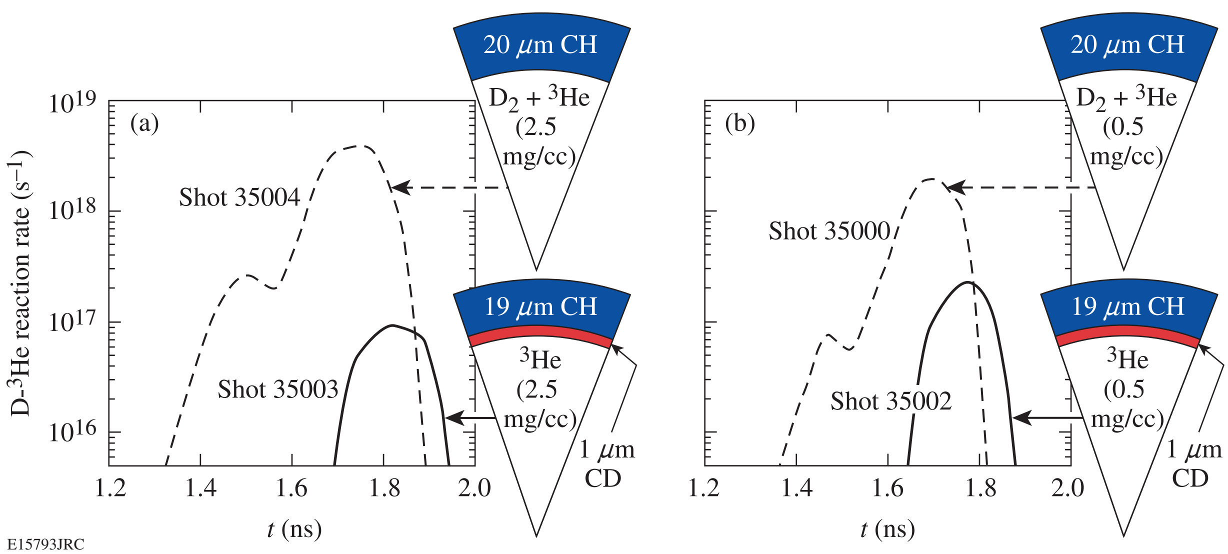

Figure 110.62
Measurements of the D-^{3}He nuclear reaction history from implosions of spherical plastic (CH) shells filled with an equimolar D_2-^{3}He mixture, and of equivalent CD-layer capsules filled with pure ^{3}He. The gaseous fuel was filled to initial densities of (a) 2.5 mg/cm^3 and (b) 0.5 mg/cm^3. The CH capsule histories show distinct times of D-^{3}He nuclear production corresponding to the shock (at ~1.5 ns) and compression (~1.75 ns) burns. CD capsule implosions require mixing of the fuel and shell on the atomic scale for D-^{3}He production, and the histories show that no such mix has occurred at shock-bang time. The time necessary for hydro-instabilities to induce fuel–shell mix results in a typical 75±30-ps delay in the peak D-^{3}He reaction rate in CD capsules compared to equivalent CH capsules. In addition, nuclear production in CD implosions continues even after the compression burn ends in CH capsules, staying well above the typical noise level of 3×10^{15}/s for an additional 50 ps.

in yields for CH capsules (see Fig. 110.62 and Table 110.X). The increase in yields for lower ρ_0 cannot be attributed to a difference in the temperature profile because both DD-n and D-^{3}He yields increased by about the same factor of 1.8, despite markedly different composition and temperature dependence. Additional mix of ^{3}He with the CD shell in low-ρ_0 implosions must be invoked to explain the yield trends.[24]

The time necessary for RT growth to induce turbulent, atomic-scale mixing of the fuel and shell results in a delay in the bang time (defined as the time of peak D-^{3}He reaction rate) of CD capsules compared to equivalent CH capsules of 83±37 ps and 69±21 ps for high and low ρ_0 (Fig. 110.63 and Table 110.X), respectively; this is equal to about half the typical 150-ps burn duration (defined as the full temporal width above half peak reaction rate). The delay is calculated as the difference between the ensemble averages of CD and CH capsule bang times, and the error is calculated as the quadrature sum of the standard errors of the mean for each ensemble average.

Measurements of DD-n bang time in CH capsules closely match the observed D-^{3}He bang time (Fig. 110.63); however, the D-D reaction rate in CD capsules was too low for robust timing measurements.

The observed bang-time delay is not an artifact of limitations of the diagnostics or experimental setup. The timing jitter of the PTD is the same for CH and CD implosions and is less than 20 ps, while bang-time errors of only 10 ps are introduced in the deconvolution process by proton energy spectrum uncertainties. A small systematic difference in shell thickness between CH and CD capsules was corrected using a 13-ps adjustment to the bang-time delay,[25] and it has been demonstrated that bang time does not depend on potential differences in implosion dynamics between capsules with pure ^{3}He fuel and capsules with D_2-^{3}He mixtures.[16]

The observed delay of the peak reaction rate for CD capsules is likely due to the difference in how mix affects nuclear production in CH and CD capsules. Whereas mix tends to quench nuclear production in CH capsules through dilution and cooling of the hot fuel, in CD capsules mix enhances nuclear production by the addition and heating of the D reactant from the shell. Nuclear production in CD capsules does not occur until later in the deceleration phase, when the growth of the RT instability has had time to induce turbulent mixing. Enhancement of reactant densities in CD capsules by continued mix in the later stages of compression, combined with the larger total

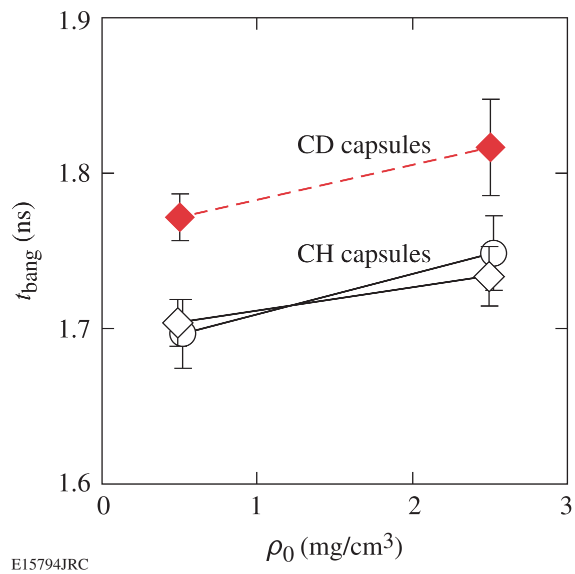

Figure 110.63
Mean and standard error of D^{3}He (diamonds) and DD-n (circles) compression-bang times from CH (open markers) and CD (solid markers) capsule implosions as a function of initial fill density. In CD capsules, D^{3}He bang time consistently occurs ~75 ps later than in CH capsules.

Table 110.X: The number of shots in different ensembles of implosions of D^{3}He-filled CH capsules and ^{3}He-filled CD capsules with two values of initial fill density ρ_0 is shown, along with ensemble averages and standard errors of the mean for several experimental observables: bang time and burn duration for DD-n and D-^{3}He nuclear reaction histories, time-integrated DD-n and D-^{3}He yields (Y_n and Y_p), and areal density ρL. Standard errors are quoted in the same units as the averages, except for the yields, which are expressed as a percent. Only the compression component is included for Y_p and ρL in CH capsules.

Type	ρ_0 (mg/cm^3)	N shots	DD bang (ps)	DD burn (ps)	D^{3}He bang (ps)	D^{3}He burn (ps)	Y_n ($\times 10^8$)	Err (%)	Y_p ($\times 10^7$)	Err (%)	ρL (mg/cm^2)
CH	2.5	8	1749±24	157±10	1734±19	155±11	129	6	61	10	54±2
CH	0.5	8	1697±22	148±11	1704±15	123±12	29	9	30	16	61±2
CD	2.5	7	—	—	1817±31	154±15	5.1	9	1.7	11	64±4
CD	0.5	5	—	—	1772±15	153±13	9.4	7	3.0	13	66±4

mass of fuel in such capsules, is enough to prolong nuclear production even after production would have been quenched in a CH implosion (Fig. 110.62).

Furthermore, systematically later nuclear production in CD capsule implosions leads to higher expected ρL. The mean radial areal density ρR increases throughout the deceleration phase as the shell continues to compress, so protons will selectively sample higher ρR (and ρL) if they are emitted later in time. This effect is in addition to the potentially higher ρL for CD capsules from geometric effects due to a noncentralized proton source profile, described above.

As seen in Fig. 110.64 and Table 110.X, ρL is 9% and 18% higher for implosions of CD capsules than for equivalent CH capsules with low and high ρ_0, respectively.[26] These values are not much higher, suggesting that one or both of the effects described above might not be as significant as expected. On this basis we conjecture that the source of protons in CD capsules may be dominated by atomic mixing at the tips of RT spikes from the shell that drive into the hot core, which would result in a more central proton emission profile and a smaller increase in ρL.

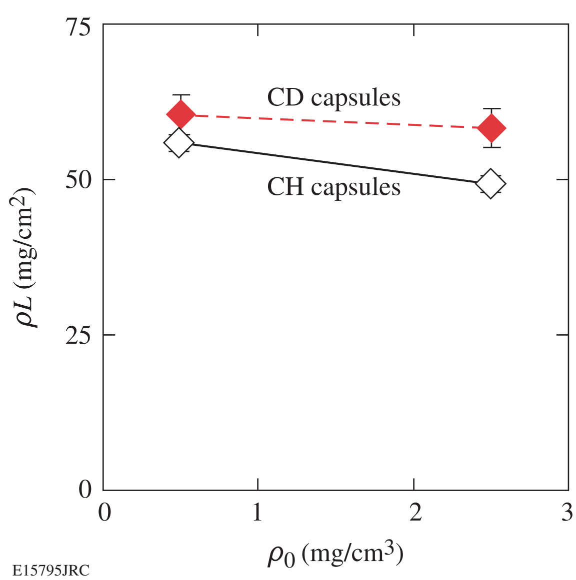

Figure 110.64
Mean and standard error of proton-emission-path–averaged areal densities (ρL) for CH (open markers) and CD (solid markers) implosions as a function of initial fill density. D^3He proton spectral measurements are used to infer this compression-burn averaged ρL, where the shock component of CH implosion spectra has been excluded. For CH capsules, the radial areal density (ρR) can be obtained from ρL using a small correction ($\rho R \sim 0.93\ \rho L$), which depends on the shell aspect ratio. The relation between ρR and ρL for CD capsules sensitively depends on the source profile as the mean source radius approaches the mean shell radius; that ρL is not much higher than in CH capsules suggests that the source profile is still centrally peaked.

In summary, temporal measurements of D^3He protons emitted from ICF implosions of CD-shell, ^3He-filled capsules offer new and valuable insights into the dynamics of turbulent mixing induced by saturation of the Rayleigh–Taylor instability. The first such measurements have demonstrated that bang time is substantially delayed as RT growth saturates to produce mix. The 83±37-ps bang-time delay of CD implosions compared to D^3He-filled, CH implosions for high initial fill densities (ρ_0) is equal to half the burn duration. Reducing ρ_0 by a factor of 5 increases the susceptibility of the implosion to mix and does not significantly affect the bang-time delay, observed to be 69±21 ps. Continued mixing of the fill gas and shell prolongs nuclear production in CD capsules even after it is quenched in equivalent CH capsules. Finally, the relatively small increase in areal density ρL of CD compared to CH capsules, despite the later bang time, suggests that nuclear production is dominated by mixing induced at the tips of RT spikes driven into the hot core.

ACKNOWLEDGMENT

The authors express their gratitude to the OMEGA engineers and operations crew who supported these experiments. This work was supported in part by the U.S. Department of Energy Office of Inertial Confinement Fusion (Grant No. DE-FG03-03NA00058), by the Lawrence Livermore National Laboratory (Subcontract No. B543881), by the Fusion Science Center for Extreme States of Matter and Fast Ignition (Contract No. 412761-G), and by the Laboratory for Laser Energetics (Subcontract No. 412160-001G) under Cooperative Agreement DE-FC52-92SF19460, University of Rochester, and New York State Energy Research and Development Authority.

REFERENCES

1. J. Nuckolls *et al.*, Nature **239**, 139 (1972).
2. S. Atzeni and J. Meyer-ter-Vehn, *The Physics of Inertial Fusion: Beam Plasma Interaction, Hydrodynamics, Hot Dense Matter*, International Series of Monographs on Physics (Clarendon Press, Oxford, 2004).
3. P. E. Dimotakis, Annu. Rev. Fluid Mech. **37**, 329 (2005).
4. See, for example, Sec. 8.9 of Ref. 2 for a review of the literature.
5. R. D. Petrasso, J. A. Frenje, C. K. Li, F. H. Séguin, J. R. Rygg, B. E. Schwartz, S. Kurebayashi, P. B. Radha, C. Stoeckl, J. M. Soures, J. Delettrez, V. Yu. Glebov, D. D. Meyerhofer, and T. C. Sangster, Phys. Rev. Lett. **90**, 095002 (2003).
6. J. R. Rygg, J. A. Frenje, C. K. Li, F. H. Séguin, R. D. Petrasso, J. A. Delettrez, V. Yu. Glebov, V. N. Goncharov, D. D. Meyerhofer, P. B. Radha, S. P. Regan, and T. C. Sangster, Phys. Plasmas **14**, 056306 (2007).

7. D. D. Meyerhofer, J. A. Delettrez, R. Epstein, V. Yu. Glebov, V. N. Goncharov, R. L. Keck, R. L. McCrory, P. W. McKenty, F. J. Marshall, P. B. Radha, S. P. Regan, S. Roberts, W. Seka, S. Skupsky, V. A. Smalyuk, C. Sorce, C. Stoeckl, J. M. Soures, R. P. J. Town, B. Yaakobi, J. D. Zuegel, J. Frenje, C. K. Li, R. D. Petrasso, D. G. Hicks, F. H. Séguin, K. Fletcher, S. Padalino, C. Freeman, N. Izumi, R. Lerche, T. W. Phillips, and T. C. Sangster, Phys. Plasmas **8**, 2251 (2001).

8. P. B. Radha, J. Delettrez, R. Epstein, V. Yu. Glebov, R. Keck, R. L. McCrory, P. McKenty, D. D. Meyerhofer, F. Marshall, S. P. Regan, S. Roberts, T. C. Sangster, W. Seka, S. Skupsky, V. Smalyuk, C. Sorce, C. Stoeckl, J. Soures, R. P. J. Town, B. Yaakobi, J. Frenje, C. K. Li, R. Petrasso, F. Séguin, K. Fletcher, S. Padalino, C. Freeman, N. Izumi, R. Lerche, and T. W. Phillips, Phys. Plasmas **9**, 2208 (2002).

9. C. K. Li, F. H. Séguin, J. A. Frenje, S. Kurebayashi, R. D. Petrasso, D. D. Meyerhofer, J. M. Soures, J. A. Delettrez, V. Yu. Glebov, P. B. Radha, F. J. Marshall, S. P. Regan, S. Roberts, T. C. Sangster, and C. Stoeckl, Phys. Rev. Lett. **89**, 165002 (2002).

10. D. C. Wilson, C. W. Cranfill, C. Christensen, R. A. Forster, R. R. Peterson, H. M. Hoffman, G. D. Pollak, C. K. Li, F. H. Séguin, J. A. Frenje, R. D. Petrasso, P. W. McKenty, F. J. Marshall, V. Yu. Glebov, C. Stoeckl, G. J. Schmid, N. Izumi, and P. Amendt, Phys. Plasmas **11**, 2723 (2004).

11. R. E. Chrien *et al*., Phys. Plasmas **5**, 768 (1998).

12. S. P. Regan, J. A. Delettrez, F. J. Marshall, J. M. Soures, V. A. Smalyuk, B. Yaakobi, V. Yu. Glebov, P. A. Jaanimagi, D. D. Meyerhofer, P. B. Radha, W. Seka, S. Skupsky, C. Stoeckl, R. P. J. Town, D. A. Haynes, Jr., I. E. Golovkin, C. F. Hooper, Jr., J. A. Frenje, C. K. Li, R. D. Petrasso, and F. H. Séguin, Phys. Rev. Lett. **89**, 085003 (2002).

13. D. C. Wilson, P. S. Ebey, A. Nobile, Jr., J. H. Cooley, T. C. Sangster, W. T. Shmayda, M. J. Bonino, D. Harding, V. Yu. Glebov, F. J. Marshall, and R. A. Lerche, Bull. Am. Phys. Soc. **51**, 295 (2006).

14. T. R. Boehly, D. L. Brown, R. S. Craxton, R. L. Keck, J. P. Knauer, J. H. Kelly, T. J. Kessler, S. A. Kumpan, S. J. Loucks, S. A. Letzring, F. J. Marshall, R. L. McCrory, S. F. B. Morse, W. Seka, J. M. Soures, and C. P. Verdon, Opt. Commun. **133**, 495 (1997).

15. S. Skupsky and R. S. Craxton, Phys. Plasmas **6**, 2157 (1999).

16. J. R. Rygg, J. A. Frenje, C. K. Li, F. H. Séguin, R. D. Petrasso, J. A. Delettrez, V. Yu. Glebov, V. N. Goncharov, D. D. Meyerhofer, S. P. Regan, T. C. Sangster, and C. Stoeckl, Phys. Plasmas **13**, 052702 (2006).

17. Non-atomic mix scenarios fail to produce significant yield since thermal ^{3}He ions cannot penetrate far enough into the CD layer. For example, to give D^{3}He yields comparable to those observed, it can be shown that all ^{3}He ions in the fuel ($\sim 2 \times 10^{17}$) would have to be launched into the CD layer at energies of 50 keV, grossly higher than the typical fuel ion temperature of 4 keV.

18. F. H. Séguin, J. A. Frenje, C. K. Li, D. G. Hicks, S. Kurebayashi, J. R. Rygg, B.-E. Schwartz, R. D. Petrasso, S. Roberts, J. M. Soures, D. D. Meyerhofer, T. C. Sangster, J. P. Knauer, C. Sorce, V. Yu. Glebov, C. Stoeckl, T. W. Phillips, R. J. Leeper, K. Fletcher, and S. Padalino, Rev. Sci. Instrum. **74**, 975 (2003).

19. *LLE Review Quarterly Report* **96**, 230, Laboratory for Laser Energetics, University of Rochester, Rochester, NY, LLE Document No. DOE/SF/19460-509, NTIS Order No. PB2006-106668 (2003).

20. J. A. Frenje, C. K. Li, F. H. Séguin, J. Deciantis, S. Kurebayashi, J. R. Rygg, R. D. Petrasso, J. Delettrez, V. Yu. Glebov, C. Stoeckl, F. J. Marshall, D. D. Meyerhofer, T. C. Sangster, V. A. Smalyuk, and J. M. Soures, Phys. Plasmas **11**, 2798 (2003).

21. R. A. Lerche, D. W. Phillion, and G. L. Tietbohl, Rev. Sci. Instrum. **66**, 933 (1995).

22. R. A. Lerche and T. J. Murphy, Rev. Sci. Instrum. **63**, 4880 (1992).

23. Or that such mix, if present, has been insufficiently heated to give nuclear production.

24. For example, if it is assumed that the DD-n yield increase is due only to an increase in the temperature of the mix region, then the fraction of ^{3}He fuel contained in the mix region must be three times greater for low ρ_0 to produce the observed D-^{3}He yield increase.

25. The 13-ps reduction in the delay corrects for a 1/3-μm systematic difference in the total thickness of the CH and CD shells, where the timing of each burn history was adjusted by (40 ps) $\times$ (20 Δ), where Δ is the capsule thickness in μm. The 40-ps/μm correction factor was obtained by a linear fit of CH capsule bang times over a range of thicknesses from 15 to 27 μm.

26. The slightly higher (<2%) initial shell mass in CD capsules due to the high density of the 1-μm-thick CD layer and the systematic thickness difference has a minimal impact on ρL (<1%).